

Criticality and the fractal structure of $-5/3$ turbulent cascades

Juan Luis Cabrera Fernández,^{1, 2, 3,*} Esther D. Gutiérrez,^{4, 2, 3} and Miguel Rodríguez Márquez^{5, 3}

¹*Departamento de Física Aplicada, ETSI Aeronáutica y del Espacio,
Universidad Politécnica de Madrid,
Pza. Cardenal Cisneros 3, 28040, Madrid, Spain*

²*Laboratorio de Dinámica Estocástica, Centro de Física,
Instituto Venezolano de Investigaciones Científicas, Caracas 1020-A, Venezuela*

³*Deeptikus Ltd., 10A Tasman Ave.,
Mount Albert, Auckland 1025, New Zealand*

⁴*Facultad de Ciencias Naturales y Matemáticas,
Escuela Superior Politécnica del Litoral,
Km 30.5 Vía Perimetral, Guayaquil, Ecuador*

⁵*Department of Biochemistry & Molecular Biology University of Calgary, T2N 4N1 Canada*

(Dated: September 9, 2022)

Abstract

In fully developed turbulence energy cascades from larger to smaller scales obeying a $-5/3$ power law. A detailed picture of the mechanism that underlies such a cascade is not known. Here we show a procedure to generate an analytical structure producing a cascade that scales as the energy spectrum in isotropic homogeneous turbulence. The procedure allows us to obtain a function that unveils a non-self-similar fractal at the origin of the cascade. It reveals that the backbone underlying cascades is formed by deterministic nested polynomials whose parameters are tuned on a critical boundary. This work shows that turbulent cascade scaling is exactly obtainable (not by numerical simulations) from deterministic low dimensional nonlinear dynamics and consequently, it should not be exclusive for fluids but probably also present in other contexts.

Keywords: Cascade, criticality, turbulence, fractals, on-off intermittency, iterated maps, nonlinear, complexity.

* juluisca@gmail.com

I. INTRODUCTION

Turbulence remains an exciting open problem. Many advances in this area have been inspired by Richardson's idea of cascades [1], Kolmogorov [2] and Onsager [3] works are excellent examples of this. However, in spite of an increasing understanding on the subject, still there isn't a detailed analytical description of the process governing energy cascading in turbulent flows. In Richardson's picture nonlinearity transforms large-scale velocity circulations (eddies) into circulations at successively smaller scales until reaching a small scale where eddies are dissipated by viscosity. Important physical insights in this picture involve the notion of inertial range [2], the derivation of the $-\frac{5}{3}$ power law energy spectrum using dimensional analysis [2, 4–7] or using the numerical simulation of shell models [8], the verification of a lack of self-similarity [9], the experiments showing the energy dissipation independence on molecular viscosity [10] or the non-Gaussian distribution of velocities and intermittency [11].

From this list, it seems interesting to note that intermittency is not exclusively observed in turbulent flows. Intermittent behavior has been noticed in many areas, and the particular type on-off intermittency - the one that we pay attention in this work - has been reported in a diverse range of problems, including nonlinear electronic circuits [12], spin-wave instabilities [13], cardiac dynamics [14], plasmas [15], econophysics [16], human stick balancing control [17], Fermi's acceleration [18], solar cycles [19] or cortical activity [20], just to name a few examples.

II. THE DRM

So, a natural question is whether it is possible to increase our knowledge of turbulent cascades analysing simple dynamical systems known to show intermittent behavior. We address this question, studying a well known low dimensional dynamics originated in population biology [25]. Let's consider an stochastic version of the delayed regulation model (DRM), given by the map on the unit interval, $x \in [0, 1]$,

$$x_{g+1} = r_g x_g (1 - x_{g-1}), \quad (1)$$

with $g = 1, \dots, +\infty$, an iteration index, $r_g = a\eta_g + b$, with η_g some random perturbation indexed by g , a , the intensity and b a bias parameter. While this analysis is not restricted

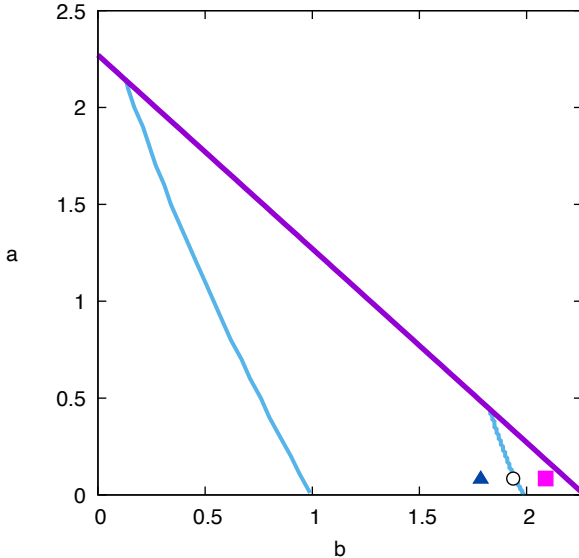


FIG. 1. Blue: boundaries for the onset of on-off intermittency for Eq. (1), calculated using the maximum Lyapunov exponent [21]. Left boundary corresponds to the origin's destabilization, the right one is for the destabilization of the fixed point $1 - \frac{1}{\langle r_g \rangle}$ via a Hopf bifurcation. Violet: stability boundary for Eq. (1) [22–24]. Points shown are located on a boundary (circle: $(0.085, 1.9375)$) and at both sides of it (triangle: $(0.085, 1.786)$, and square: $(0.085, 2.089)$) and will be used below.

to a particular distribution of η_g , for simplicity sake we assume the simplest case with η_g uniformly distributed on $[0, 1]$, so that $r_g \in [b, a + b]$. For the case of zero delay and zero noise, the map (1) is the well known deterministic logistic map. Eq. (1) is probably one of the simplest dynamical systems containing nonlinearities, time delayed feedback and parametric random perturbations. The deterministic counterpart of Eq. (1) has been widely studied [22, 26, 27] and its non-deterministic version has been used to analyze stochastic extinctions [23, 24], autonomous stochastic resonance [28] and noise-induced localization [29]. Eq. (1) shows sustained on-off intermittency for parameter values a and b tuned at the boundaries displayed in figure 1. A first boundary is for the onset of intermittency caused by destabilization of the origin and a second boundary in for the onset of intermittency by destabilization of the fixed point $1 - 1/\langle r_g \rangle$. We will work on this second boundary because it allows for intermittent signals consisting of bursts involving stochastic limit cycle oscillations. as the DRM undergoes a Hopf bifurcation at $r_H = 2$ [22, 23].

III. LINEALIZATION OF THE DRM

In the following we will use the noise to facilitate the calculations that will allow us to obtain important results. Later these results will be analyzed with the noise off. A first step is linearizing Eq. (1) which can be rewritten as

$$x_{g+1} = r_g F(x_g, y_g) \quad (2)$$

$$y_{g+1} = G(x_g, y_g) \quad (3)$$

with $F(x, y) \equiv x(1 - y)$ and $G(x, y) \equiv x$. F and G can be expanded around the fixed point $P \equiv (\alpha, \alpha)$ with $\alpha \equiv 1 - \frac{1}{\langle r_g \rangle} \equiv 1 - \frac{1}{\beta}$, to obtain,

$$F(x, y) = F(\alpha, \alpha) + (x - \alpha) \frac{\partial F}{\partial x} \Big|_P + (y - \alpha) \frac{\partial F}{\partial y} \Big|_P + O(x^2, y^2) \quad (4)$$

$$G(x, y) = G(\alpha, \alpha) + (x - \alpha) \frac{\partial G}{\partial x} \Big|_P + (y - \alpha) \frac{\partial G}{\partial y} \Big|_P + O(x^2, y^2), \quad (5)$$

i.e.,

$$F(x, y) = \alpha^2 + (1 - \alpha)x - \alpha y \quad (6)$$

$$G(x, y) = x. \quad (7)$$

Close to the fixed point P , Eq. (1) can be approximated by its linear part:

$$x_{g+1} = r_g \left(\alpha^2 + \frac{x_g}{\beta} - \alpha y_g \right) \quad (8)$$

$$y_{g+1} = x_g \quad (9)$$

It is better to rewrite it as,

$$\begin{pmatrix} x \\ y \end{pmatrix}_{g+1} = \begin{pmatrix} r_g/\beta & -\alpha r_g \\ 1 & 0 \end{pmatrix} \begin{pmatrix} x \\ y \end{pmatrix}_g + \begin{pmatrix} \alpha^2 r_g \\ 0 \end{pmatrix}. \quad (10)$$

It allows us to define the evolution matrix:

$$\mathbf{A}_g \equiv \begin{pmatrix} r_g/\beta & -\alpha r_g \\ 1 & 0 \end{pmatrix} \quad (11)$$

and the bias vector:

$$\vec{B}_g \equiv \begin{pmatrix} \alpha^2 r_g \\ 0 \end{pmatrix}. \quad (12)$$

Then Eq. (10) can be compacted as,

$$\vec{X}_{g+1} = \mathbf{A}_g \vec{X}_g + \vec{B}_g. \quad (13)$$

IV. EXPANDING \vec{X}_g

It is useful to express \vec{X}_g in terms of the initial state \vec{X}_0 . So, let's note that \vec{X}_{g+1} can be patiently expanded as follows,

$$\begin{aligned}
\vec{X}_{g+1} &= \mathbf{A}_g \vec{X}_g + \vec{B}_g \\
&= \mathbf{A}_g (\mathbf{A}_{g-1} \vec{X}_{g-1} + \vec{B}_{g-1}) + \vec{B}_g \\
&= \mathbf{A}_g (\mathbf{A}_{g-1} (\mathbf{A}_{g-2} \vec{X}_{g-2} + \vec{B}_{g-2}) + \vec{B}_{g-1}) + \vec{B}_g \\
&\quad \vdots \\
&= \mathbf{A}_g \mathbf{A}_{g-1} \mathbf{A}_{g-2} \mathbf{A}_{g-3} \dots \mathbf{A}_1 \mathbf{A}_0 \vec{X}_0 \\
&+ \mathbf{A}_g \mathbf{A}_{g-1} \mathbf{A}_{g-2} \mathbf{A}_{g-3} \dots \mathbf{A}_1 \vec{B}_0 \\
&\quad \vdots \\
&+ \mathbf{A}_g \mathbf{A}_{g-1} \mathbf{A}_{g-2} \vec{B}_{g-3} \\
&+ \mathbf{A}_g \mathbf{A}_{g-1} \vec{B}_{g-2} \\
&+ \mathbf{A}_g \vec{B}_{g-1} \\
&+ \vec{B}_g
\end{aligned} \tag{14}$$

Then, \vec{X}_{g+1} can be written as,

$$\begin{aligned}
\vec{X}_{g+1} &= \prod_{j=0}^g \mathbf{A}_{g-j} \vec{X}_0 \\
&+ \prod_{j=0}^{g-1} \mathbf{A}_{g-j} \vec{B}_0 \\
&+ \prod_{j=0}^{g-2} \mathbf{A}_{g-j} \vec{B}_1 \\
&+ \prod_{j=0}^{g-3} \mathbf{A}_{g-j} \vec{B}_2 \\
&\quad \vdots \\
&+ \prod_{j=0}^{g-(g-2+1)=1} \mathbf{A}_{g-j} \vec{B}_{g-2} \\
&+ \prod_{j=0}^{g-(g-1+1)=0} \mathbf{A}_{g-j} \vec{B}_{g-1} \\
&+ \vec{B}_g \\
&= \prod_{j=0}^g \mathbf{A}_{g-j} \vec{X}_0
\end{aligned}$$

$$+ \sum_{i=1}^{g+1} \prod_{j=0}^{g-i} \mathbf{A}_{g-j} \vec{B}_{i-1}. \quad (15)$$

Where we are using the definition,

$$\prod_{j=0}^{g-i} \mathbf{A}_{g-j} \equiv 1 \text{ if } i = g+1. \quad (16)$$

Now, changing variables, $g \rightarrow g' - 1$, we obtain,

$$\vec{X}_g = \prod_{j=0}^{g-1} \mathbf{A}_{g-j-1} \vec{X}_0 + \sum_{i=1}^g \prod_{j=0}^{g-i-1} \mathbf{A}_{g-j-1} \vec{B}_{i-1}, \quad (17)$$

where we have omitted the prime and used,

$$\prod_{j=0}^{g-i-1} \mathbf{A}_{g-j-1} \equiv \mathbf{1} \text{ if } i = g. \quad (18)$$

Thus, we can define,

$$\mathbf{P}_i \equiv \prod_{j=0}^{g-i-1} \mathbf{A}_{g-j-1} \quad \text{if } i \neq g, \quad (19)$$

$$\mathbf{P}_i \equiv \mathbf{1} \quad \text{if } i = g,$$

$$\mathbf{P}_g \equiv \prod_{j=0}^{g-1} \mathbf{A}_j, \quad (20)$$

to write \vec{X}_g in a compact form,

$$\vec{X}_g = \mathbf{P}_g \vec{X}_0 + \sum_{i=1}^g \mathbf{P}_i \vec{B}_{f(i)}, \quad (21)$$

with $f(i) \equiv i - 1$.

V. SIMPLIFYING $\vec{X}_g = \mathbf{P}_g \vec{X}_0 + \sum_{i=1}^g \mathbf{P}_i \vec{B}_{f(i)}$

For convenience in the following calculations are on the complex plane. Let be \vec{Y}_g a state at generation g obtained with a realization $r'_g \neq r_g$. Calculating the dot product of \vec{X}_g and \vec{Y}_g gives,

$$\vec{X}_g \cdot \vec{Y}_g = \mathbf{P}_g \vec{X}_0 \cdot \vec{Y}_g + \sum_{i=1}^g \mathbf{P}_i \vec{B}_{f(i)} \cdot \vec{Y}_g. \quad (22)$$

The scalar quantity $\eta_g \equiv \vec{X}_g \cdot \vec{Y}_g$ is the value for the projection of \vec{X}_g onto \vec{Y}_g . It is a random variable evaluated at generation g , that takes values on the interval $[0, 1]$. Also, let's note that applying the operator \mathbf{P}_g on the initial condition \vec{X}_0 , produces a new state

at generation g , say $\vec{\mu}_g$. Thus, the dot product between $\mathbf{P}_g \vec{X}_0 = \vec{\mu}_g$ and \vec{Y}_g yields also a scalar random variable at generation g , say $0 \leq \psi_g \leq 1$, i.e.,

$$\mathbf{P}_g \vec{X}_0 \cdot \vec{Y}_g = \vec{\mu}_g \cdot \vec{Y}_g \equiv \psi_g \quad (23)$$

With these considerations in mind we can rewrite Eq. (22) as,

$$\begin{aligned} \eta_g &= \psi_g + \sum_{i=1}^g \mathbf{P}_i \vec{B}_{f(i)} \cdot \vec{Y}_g \\ &= \psi_g \left(1 + \psi_g^{-1} \sum_{i=1}^g \mathbf{P}_i \vec{B}_{f(i)} \cdot \vec{Y}_g \right). \end{aligned} \quad (24)$$

After rearranging terms, it results in,

$$\psi_g \left(\frac{\eta_g}{\psi_g} - 1 \right) = \sum_{i=1}^g \mathbf{P}_i \vec{B}_{f(i)} \cdot \vec{Y}_g \quad (25)$$

or

$$\left(\frac{\eta_g}{\psi_g} - 1 \right) \vec{\mu}_g \cdot \vec{Y}_g = \sum_{i=1}^g \mathbf{P}_i \vec{B}_{f(i)} \cdot \vec{Y}_g, \quad (26)$$

where we have used Eq. (23). This expression is the same as,

$$\left\{ \left(\frac{\eta_g}{\psi_g} - 1 \right) \vec{\mu}_g - \sum_{i=1}^g \mathbf{P}_i \vec{B}_{f(i)} \right\} \cdot \vec{Y}_g = 0. \quad (27)$$

Now, at a given step, g , this equation has two possible consequences: i) either the vectors, $\left(\left(\frac{\eta_g}{\psi_g} - 1 \right) \vec{\mu}_g - \sum_{i=1}^g \mathbf{P}_i \vec{B}_{f(i)} \right)$ and \vec{Y}_g , are orthogonal vectors, in which case its dot product would equals zero, or ii) the following equality is satisfied,

$$\left(\frac{\eta_g}{\psi_g} - 1 \right) \vec{\mu}_g = \sum_{i=1}^g \mathbf{P}_i \vec{B}_{f(i)}, \quad (28)$$

In what follows, we assume that condition ii) predominates, i.e., that the involved random dynamics reduces the probability of i) to a minimum, such that most of the evolution of the system can be better characterized by condition ii) at least in $O(\{\left(\frac{\eta_g}{\psi_g} - 1 \right) \vec{\mu}_g - \sum_{i=1}^g \mathbf{P}_i \vec{B}_{f(i)}\} \cdot \vec{Y}_g)$. That being said, we must also impose $b > 1$ to avoid the case $r_g < 1$ if $\eta_g = 0$, which would take the system state to the zero fixed point, a situation where we can't rule out $\vec{Y}_g = 0$, at least momentarily. With these thoughts in mind, and using the definition of $\vec{\mu}_g$, condition ii) turns out as,

$$\left(\frac{\eta_g}{\psi_g} - 1 \right) \mathbf{P}_g \vec{X}_0 = \sum_{i=1}^g \mathbf{P}_i \vec{B}_{f(i)}, \quad (29)$$

a relation that we can introduce into Eq. (21), to obtain a shorter expression for the time evolution of the system in terms of the product \mathbf{P}_g ,

$$\begin{aligned}
\vec{X}_g &= \mathbf{P}_g \vec{X}_0 + \left(\frac{\eta_g}{\psi_g} - 1 \right) \mathbf{P}_g \vec{X}_0, \\
&= \frac{\eta_g}{\psi_g} \mathbf{P}_g \vec{X}_0 \\
&= \gamma_g \mathbf{P}_g \vec{X}_0 \\
&= \mathbf{P}'_g \vec{X}_0.
\end{aligned} \tag{30}$$

Here, $\gamma_g \equiv \frac{\eta_g}{\psi_g}$, is a random number and $\mathbf{P}'_g \equiv \gamma_g \mathbf{P}_g$ is the original product modulated by γ_g . To know the range of values that γ_g takes, let's consider the inequality:

$$0 \leq \mathbf{P}_g \vec{X}_0 \cdot \vec{Y}_g < \mathbf{P}_g \vec{X}_0 \cdot \vec{Y}_g + \sum_{i=1}^g \mathbf{P}_i \vec{B}_{f(i)} \cdot \vec{Y}_g = \vec{X}_g \cdot \vec{Y}_g \leq 1 \tag{31}$$

or

$$0 \leq \mathbf{P}_g \vec{X}_0 \cdot \vec{Y}_g < \vec{X}_g \cdot \vec{Y}_g \leq 1, \tag{32}$$

i.e.,

$$0 \leq \psi_g < \eta_g \leq 1. \tag{33}$$

Then,

$$1 < \gamma_g < \infty. \tag{34}$$

Therefore, γ_g is an unbounded random variable larger than 1, i.e., applying γ_g on \mathbf{P}_g has an amplifying effect.

VI. CALCULATING THE NORM OF \vec{X}_g

At this point, we would like to know about how the norm of \vec{X}_g behaves. It can be determined by calculating the inner product,

$$\| \vec{X}_g \| = [\vec{X}_g^* \vec{X}_g]^{1/2} = [\vec{X}_0 \mathbf{P}'_g \mathbf{P}'_g \vec{X}_0]^{1/2}, \tag{35}$$

given that \mathbf{P}'_g is not a self-adjoint operator. Here \mathbf{P}'_g^\dagger is the Hermitian conjugate of the operator \mathbf{P}'_g , i.e., the adjoint matrix in our case. Then, the problem of calculating the norm

translates to the calculation of $\mathbf{P}'^\dagger \mathbf{P}'_g$. To evaluate such a product we must write it in terms of the time dependent random matrix \mathbf{A}_g ,

$$\mathbf{P}'^\dagger \mathbf{P}'_g = \gamma_g^* \mathbf{P}_g^\dagger \gamma_g \mathbf{P}_g = \gamma_g^* \gamma_g \mathbf{P}_g^\dagger \mathbf{P}_g, \quad (36)$$

where

$$\begin{aligned} \mathbf{M}_g \equiv \mathbf{P}_g^\dagger \mathbf{P}_g &= [\mathbf{A}_{g-1} \mathbf{A}_{g-2} \dots \mathbf{A}_1 \mathbf{A}_0]^\dagger \mathbf{A}_{g-1} \mathbf{A}_{g-2} \dots \mathbf{A}_1 \mathbf{A}_0 = \\ &= \mathbf{A}_0^\dagger \mathbf{A}_1^\dagger \dots \mathbf{A}_{g-2}^\dagger \mathbf{A}_{g-1}^\dagger \mathbf{A}_{g-1} \mathbf{A}_{g-2} \dots \mathbf{A}_1 \mathbf{A}_0 = \\ &= \mathbf{A}_0^\dagger [\mathbf{A}_1^\dagger \dots [\mathbf{A}_{g-2}^\dagger [\mathbf{A}_{g-1}^\dagger \mathbf{A}_{g-1}] \mathbf{A}_{g-2}] \dots \mathbf{A}_1] \mathbf{A}_0, \end{aligned} \quad (37)$$

and

$$\mathbf{A}_g^\dagger = \begin{pmatrix} r_g/\beta & 1 \\ -r_g\alpha & 0 \end{pmatrix} \quad (38)$$

VII. EIGENVALUES OF p_1

A straightforward evaluation of \mathbf{M}_g doesn't seem possible. However, we can address attention on how it evolves step by step. In particular, in the equation for \mathbf{M}_g , the core or first product is given by:

$$p_1 \equiv \mathbf{A}_{g-1}^\dagger \mathbf{A}_{g-1} = \begin{pmatrix} \frac{r_1^2 + \beta^2}{\beta^2} & -\frac{r_1^2}{\beta} \alpha \\ -\frac{r_1^2}{\beta} a & \alpha^2 r_1^2 \end{pmatrix}, \quad (39)$$

where we are using the notation $r_i \equiv r_{g-i}$. It should be noted that this matrix has eigenvalues,

$$\lambda_{\pm}^{p_1} = \frac{1}{2\beta^2} \left((1 + \alpha^2 r_1^2) \beta^2 + r_1^2 \pm \sqrt{((1 + \alpha^2 r_1^2) \beta^2 + r_1^2)^2 - (2\alpha\beta^2 r_1)^2} \right). \quad (40)$$

So, the eigenvalues of the product p_1 can be expressed as,

$$\lambda_{\pm}^{p_1} = \frac{1}{2\beta^2} \left(\Lambda_1 \pm \sqrt{\Lambda_1^2 - \Upsilon_1^2} \right). \quad (41)$$

where, $\Lambda_1 \equiv (1 + \beta^2 \alpha^2) r_1^2 + \beta^2$, and $\Upsilon_1 \equiv 2\beta^2 \alpha r_1$. This process is repeated to calculate the next product, $p_2 \equiv \mathbf{A}_{g-2}^\dagger p_1 \mathbf{A}_{g-2}$, and similarly, p_3 , and so on. A detailed account of these calculations is provided in the appendixes A-D. From there, it is clear that the eigenvalues

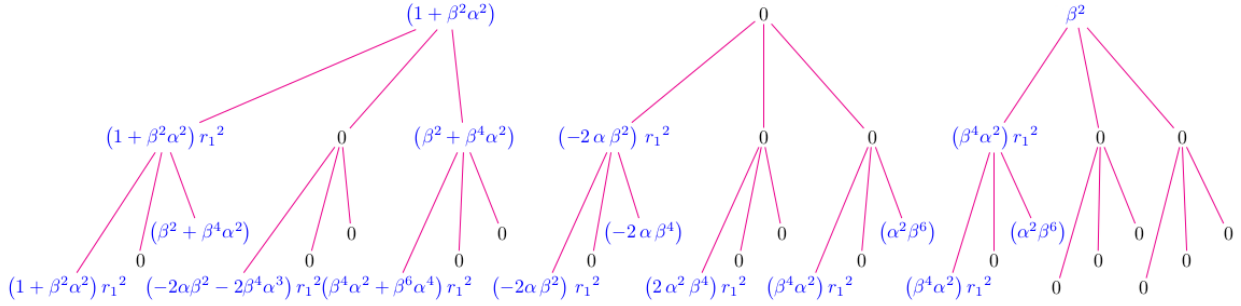


FIG. 2. Tree representation for the generation of the polynomial coefficients after two iterations of rule (49, 50), starting from Λ_1 . Bottom coefficients are those forming Λ_3 given by Eq. (B3).

for the first five products can be expressed as:

$$\lambda_{\pm}^{p_2} = \frac{1}{2\beta^4} \left(\Lambda_2 \pm \sqrt{\Lambda_2^2 - \Upsilon_2^2} \right) \quad (42)$$

$$\lambda_{\pm}^{p_3} = \frac{1}{2\beta^6} \left(\Lambda_3 \pm \sqrt{\Lambda_3^2 - \Upsilon_3^2} \right) \quad (43)$$

$$\lambda_{\pm}^{p_4} = \frac{1}{2\beta^8} \left(\Lambda_4 \pm \sqrt{\Lambda_4^2 - \Upsilon_4^2} \right) \quad (44)$$

$$\lambda_{\pm}^{p_5} = \frac{1}{2\beta^{10}} \left(\Lambda_5 \pm \sqrt{\Lambda_5^2 - \Upsilon_5^2} \right) \quad (45)$$

where the definitions for Λ_i and Υ_i are given in the appendixes.

VIII. NESTED STRUCTURES

The previous section allows us to infer how the eigenvalues evolve with each generation g . In particular, eigenvalues for each product, p_1, p_2, \dots, p_N , can be written as,

$$\lambda_{\pm}^{p_g} = \frac{1}{2\beta^{2g}} \left(\Lambda_g \pm \sqrt{\Lambda_g^2 - \Upsilon_g^2} \right), \quad (46)$$

where terms Λ_g and Υ_g are polynomials in the noise terms, i.e., random polynomials. In particular, Υ_g , can be easily written in compact form as,

$$\Upsilon_g = 2\beta^{2g}\alpha^g \prod_{i=1}^g r_i. \quad (47)$$

However, a closed form for Λ_g is not so immediate. It is so because Λ_g follows a complex nested structure as illustrated in the appendixes. One must note that Λ_g is a polynomial in r_g of order two, whose coefficients are polynomials of order two in r_{g-1} , whose coefficients

are polynomials of order two in r_{g-2} , and so on. Let's say that $C(r_{g-1}, \dots, r_1)$ is a function that depends on the noise terms r_{g-1}, \dots, r_1 , and that such a function is a coefficient of a noise term of order i , i.e., that given a second order polynomial describing Λ_g it has terms $C_i(r_{g-1}, \dots, r_1)r^i$. Now, depending on what Λ_g are we dealing with, we shall distinguish each of these functional coefficients. Consequently, it is convenient indexing also the C 's to make such a distinction, so writing these terms as $C_{g,i}(r_{g-1}, \dots, r_1)r_g^i$. Here, we have also indexed r_g , because that noise's value is exactly the one at step g . Accordingly, Λ_g can be conveyed to,

$$\Lambda_g = \sum_{i=0}^2 C_{g,i}(r_{g-1}, \dots, r_1)r_g^i \quad (48)$$

with $C_{1,i} \equiv C_{g,i}(r_{g-1}, \dots, r_1)|_{g=1}$, constant. Note that we have not indexed the coefficients of the nested levels because there is no need for that, we try to keep the notation simple, as far as possible. Now, let's reproduce the full structure as follows. In general, if we know Λ_1 and Λ_2 , we can obtain Λ_g given that, in the generation $g-1$, a given term,

$$\{C_2 r_i^2 + C_1 r_i + C_0\} r_{i+1}^k \quad \text{with } k = 0, 1, 2, \quad (49)$$

generates the polynomial,

$$\left\{ \begin{array}{l} [C_2 r_i^2 + C_1 \chi_1 r_i + \beta^2 C_2] r_{i+1}^2 \\ + [-k\alpha\beta^2 C_2 r_i^2 + C_1 \chi_2 r_i + C_1 \chi_3] r_{i+1} \\ + [\beta^2 \alpha^2 C_0 r_i^2 + C_1 \chi_4 r_i + C_1 \chi_5] \end{array} \right\} r_{i+2}^k, \quad (50)$$

in the next generation, g . $\chi_1, \chi_2, \dots, \chi_5$ are unknowns, here included to stress the polynomial nested structure, but multiplied by C_1 , that in the present situation vanishes.

IX. GENERATING NESTED ESTRUCTURES: AN EXAMPLE

The preceding procedure is better illustrated with an example: finding Λ_3 from Λ_2 , which is given by Eq. (A3). The coefficient for the quadratic term is, $[(1 + \alpha^2\beta^2)r_1^2 + \beta^2(1 + \alpha^2\beta^2)]$, therefore, $C_2 = 1 + \alpha^2\beta^2$, $C_1 = 0$ and $C_0 = \beta^2(1 + \alpha^2\beta^2)$; and the quadratic term in r_3 is generated as,

$$\left\{ \begin{array}{l} [(1 + \alpha^2\beta^2)r_1^2 + \beta^2(1 + \alpha^2\beta^2)] r_2^2 \\ + [-2\alpha\beta^2(1 + \alpha^2\beta^2)r_1^2] r_2 \\ + [\beta^4\alpha^2(1 + \alpha^2\beta^2)r_1^2] \end{array} \right\} r_3^2. \quad (51)$$

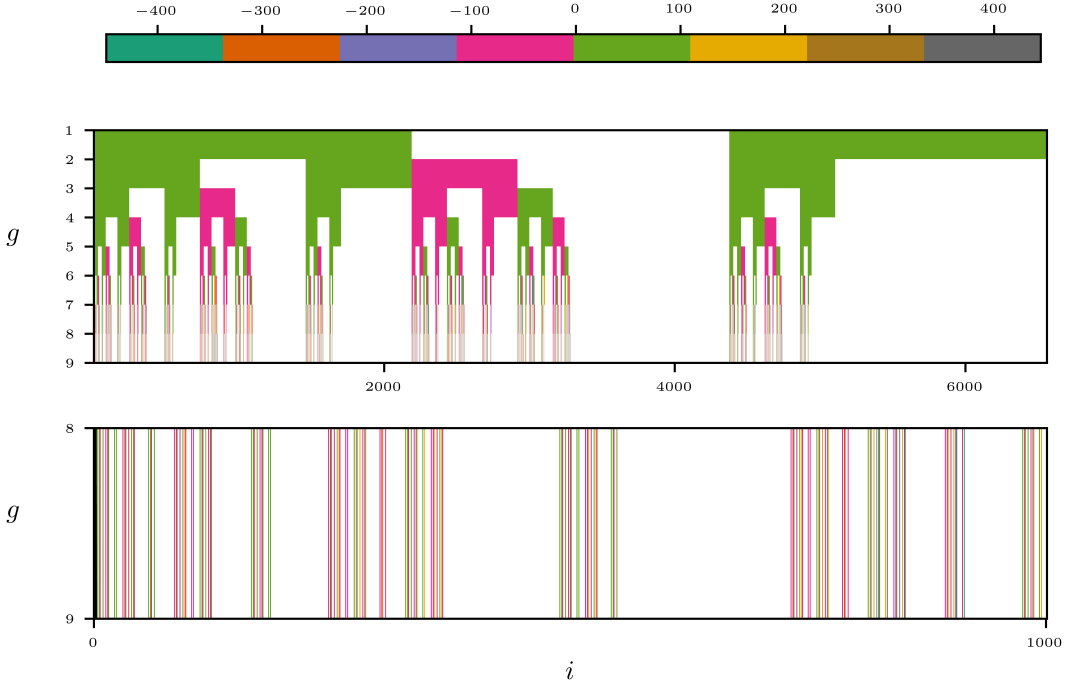


FIG. 3. (Top) Analytical deterministic cascade describing the evolution of the nested polynomial coefficients C_2 , C_1 and C_0 (from left to right) after $n = 8$ iterations. Colors represent the coefficient's intensities a_i . The iteration process starts with the Λ_1 coefficients, each one laying on $\frac{1}{3}$ segments on the x -axis which hosts 3^8 subdivisions. (Bottom) Zoom in the interval $[0, 1000]$ showing fine structure. Parameter values are $r = 1$ and (a, b) as in the circle point on the boundary at figure 1.

Now, the lineal term in Λ_2 is $-2\alpha\beta^2r_1^2$, therefore in this case, $C_2 = -2\alpha\beta^2$ and $C_1 = C_0 = 0$. Then the linear term in r_3 is,

$$\left\{ \begin{array}{l} [(-2\alpha\beta^2)r_1^2 + (-2\alpha\beta^4)]r_2^2 \\ + [2\alpha^2\beta^4r_1^2]r_2 \end{array} \right\} r_3. \quad (52)$$

Finally, the coefficient of the independent term in Λ_2 is $(\alpha^2\beta^4)r_1^2$. Then $C_2 = \alpha^2\beta^4$ and $C_1 = C_0 = 0$, so we obtain,

$$\left\{ [(\alpha^2\beta^4)r_1^2 + \alpha^2\beta^6]r_2^2 \right\} r_3^0. \quad (53)$$

Adding Eq. (51), (52) and (53) results in Λ_3 .

X. DETERMINING THE LEADING TERM IN λ

The eigenvalues of \mathbf{M}_g are given by Eq. (46) with the term Υ_g growing as a power of the noise term, i.e., $\Upsilon_g \sim r^g$. Meanwhile, the equations (VII), (A3), (B3), (C3) and (D3) indicate that the Λ_g 's grow as a sum of powers in the noise, i.e.,

$$\begin{aligned}\Lambda_1 &\sim r^2 \\ \Lambda_2 &\sim r^4 + r^3 + r^2 \\ \Lambda_3 &\sim r^6 + r^5 + r^4 + r^3 + r^2 \\ \Lambda_4 &\sim r^8 + r^7 + r^6 + r^5 + r^4 \\ \Lambda_5 &\sim r^{10} + \dots + r^4.\end{aligned}\tag{54}$$

So, $\Lambda_g > \Upsilon_g$ and Λ_g will predominate for g sufficiently large, i.e., $\frac{\Upsilon_g}{\Lambda_g} \rightarrow 0$, thus Eq. (46) yields,

$$\begin{aligned}\lambda_+^{pg} &\sim \Lambda_g + O\left(\frac{\Upsilon_g}{\Lambda_g}\right) \\ \lambda_-^{pg} &\sim 0 + O\left(\frac{\Upsilon_g}{\Lambda_g}\right)\end{aligned}\tag{55}$$

Let's unpack Eq. (35) to determine the implications of this approximation on the norm $\|\vec{X}_g\|$,

$$\begin{aligned}\|\vec{X}_g\| &= (\gamma_g^* \gamma_g \vec{X}_0^* \mathbf{M}_g \vec{X}_0)^{1/2} \\ &= \gamma_g \left[(x_0 y_0) \begin{pmatrix} \lambda_+ & 0 \\ 0 & \lambda_- \end{pmatrix} \begin{pmatrix} x_0 \\ y_0 \end{pmatrix} \right]^{\frac{1}{2}}.\end{aligned}\tag{56}$$

Combining this equation with the Eqs. (55) we find that Λ_g leads the behavior of the norm,

$$\|\vec{X}_g\| \sim \frac{\gamma_g}{\beta^g} \sqrt{\Lambda_g} x_0.\tag{57}$$

XI. A HIDDEN FRACTAL STRUCTURE

The hidden structure of the Λ_g 's is better understood using a graphical representation. figure 2 shows the branching process obtained after three iterations of the rule (49, 50). The terms displayed at the bottom are the coefficients of Λ_3 (see Appendix B). This representation reveals a cascading process at the backbone of the eigenvalues time evolution. To

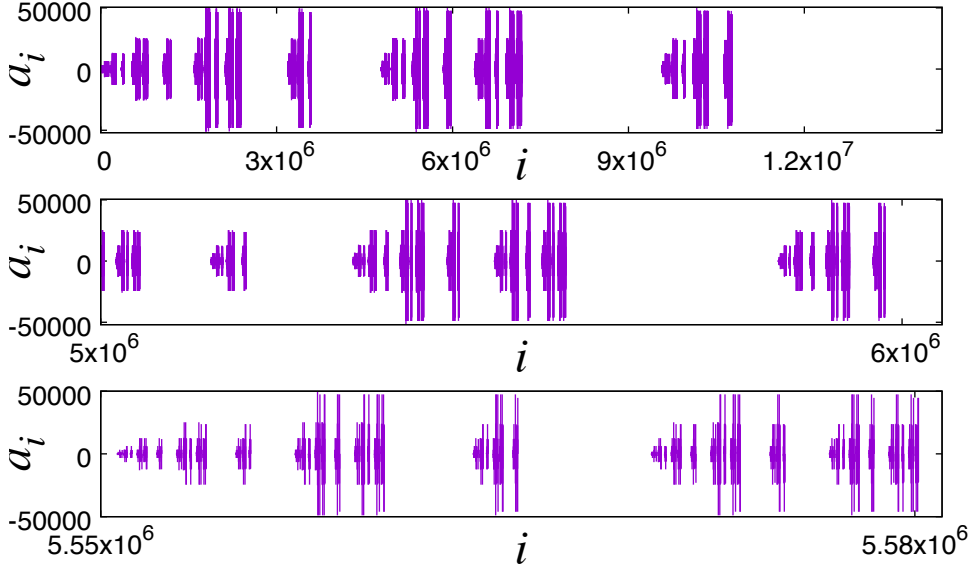


FIG. 4. Non-self-similar structure of the analytical deterministic cascade revealed after successive enlargements. Image obtained with $g = 15$ generations and parameter values as in figure 3. The number of coefficients calculated is $3^{15} = 14.348.907$. Points are represented by impulses and zero ones have been extracted.

get a deeper insight into such a structure we will focus exclusively on the evolution of the coefficients described in figure 2, turning off any random influence. It is achieved arbitrarily considering $r_g = r$ a constant, conveniently established as $r = 1, \forall g$. However, such a deterministic constrain still depends on constants a and b which will be properly chosen, such that the system evolves close to the Hopf bifurcation. Under these conditions the cascade obtained is depicted in figure 3. The method used to obtain this figure is the following: the coefficient values in the initial polynomial Λ_1 , i.e., C_2, C_1 and C_0 , define branch intensities, $a_i, i = 1, 2, 3$, on the $N_1 = 3^1$ subintervals of the unit interval: $I_2 \equiv [0, \frac{1}{3})$, $I_1 \equiv [\frac{1}{3}, \frac{2}{3})$ and $I_0 \equiv [\frac{2}{3}, 1]$, respectively. After one iteration, each subset is divided by a factor of 3, and the newly generated coefficients - obtained using rule (49, 50). - shall update the a_i 's on new $N_2 = 3^2$ subintervals. After each new generation, the unit interval is divided by a factor of 3 such that, after g iterations, the value of the coefficients can be represented as intensities on $N_g = 3^g$ subintervals, given by rule (49, 50). figure 3 exposes how fast the cascade grows: after $g = 8$ generations, the unit interval harbours $N_8 \sim 3^8 = 6561$ coefficients on the same number of subintervals. Because $r_g = 1, \forall g$, this fractal cascade is the support for random perturbations to shape the norm of \vec{X}_g or other quantities based on it. The bottom part

of figure 3 shows a detail of the fine structure of this object. I_2 is the only segment that obeys a self-similar rule, given by $X_{g+1} = \frac{X_g}{3}$; $X \in I = [0, 1]$. Subintervals I_1 and I_0 don't seem to follow a self-similar rule. The mapping process shows an independent progression for each of the initial I_i intervals, yielding a non-self-similar structure with multifractal characteristics whose full characterization will be carried out elsewhere. Branch intensities a_i , $i = 1 \dots 3^g$, display a nontrivial behaviour as seen in figure 4. We plotted a_i for each branch on the limit set after $g = 15$ iterations. The horizontal axis contains $N_{15} = 3^{15} = 14.348.907$ points. Successive enlargements of the initial interval show statistically equivalent objects as expected for a fractal. The figure also shows that the lack of self-similarity extends to both, the branch positions and their intensities. The behavior of the distribution of intensities (figure 5) is comparable with Thomae's self-similar function as has been reported also for high-throughput biological and clinical data [30].

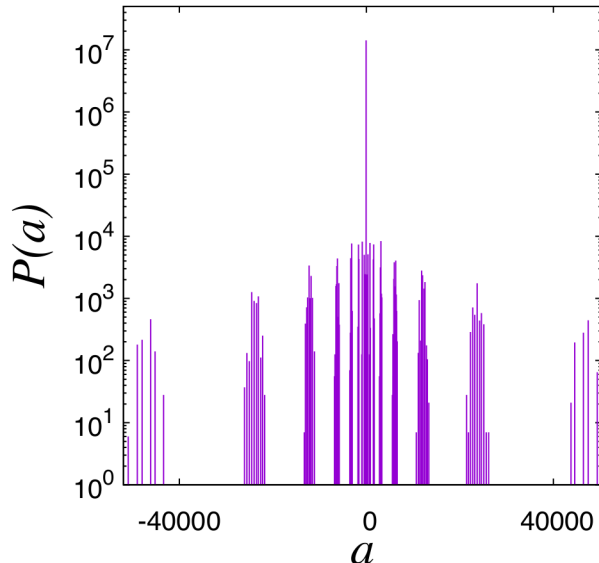


FIG. 5. Semi-log plot of the intensity distribution from the deterministic cascade obtained after 15 generations. Same parameter values as in figure 3.

XII. CASCADING SCALING BEHAVIOUR

So far, except for using the term cascade to describe successive iterations of rule (49, 50), we haven't shown any link with cascades in turbulence phenomena. To establish such a bridge, we must conjecture some sort of parallel between the intensities a_i and the energy by

wave number. The idea behind is that, if a_i is a main changing quantity from the cascading rule (49, 50), it could be related with a main changing quantity in turbulent cascades: the energy, i.e.,

$$E(k) \sim E(g). \quad (58)$$

Thus, if there are l_g non-zero intensities at a scale g , we define an energy measure at generation step g by the relation:

$$E(l_g) \equiv \left(\sum_{\forall a_i \neq 0} |a_i(l_g)| \right)^{-1}, \quad (59)$$

i.e., the inverse value of the summation of the magnitude for all intensities at scale g . Circles shown in figure 6 describe the behaviour of this quantity as a function of the scale in a deterministic cascade as the one illustrated in figure 3, obtained with the parameter values on the on-off intermittency boundary at figure 1. It can be seen that these points follow a $-5/3$ power law over six orders of magnitude. This is the same power law found for the energy spectrum in fully developed isotropic homogeneous turbulence [31] and deduced by Kolmogorov [2]. Therefore, $E(l_g)$ scales following the expected law for turbulent cascades,

$$E(l_g) \sim l_g^{-\frac{5}{3}}. \quad (60)$$

From this relation, it is straightforward to identify l_g with the wave number k , i.e., $l \sim k$. Thus, assumption (58) can be explicitly written as,

$$E(k) \sim E(l_g) \sim l_g^{-\frac{5}{3}}. \quad (61)$$

When the parameter values are distant from the on-off boundary, the calculated $E(l_g)$ deviates from the $-\frac{5}{3}$ power law, as is shown in figure 6. The cascading rule (49, 50) resembles a turbulent cascade exclusively when the parameters $(a + b)$ are almost tuned on the Hopf bifurcation critical point and such resemblance disappears when the parameters are moved away from it. This result emphasizes a critical and deterministic origin of the cascade's $-5/3$ power law. Our results suggest that in this deterministic situation, the cascade would continue without end, meaning that increasing g to a much larger value shall still produce the $-5/3$ law, in which case one could assume that the inertial range extends to infinity. Such an assumption is in line with the Onsager's conjecture that dissipation energy might exist even in the limit of vanishing viscosity [3, 5]. Additionally, an interesting characteristic of the cascade reported here is that it is rooted in an apparently multifractal structure.

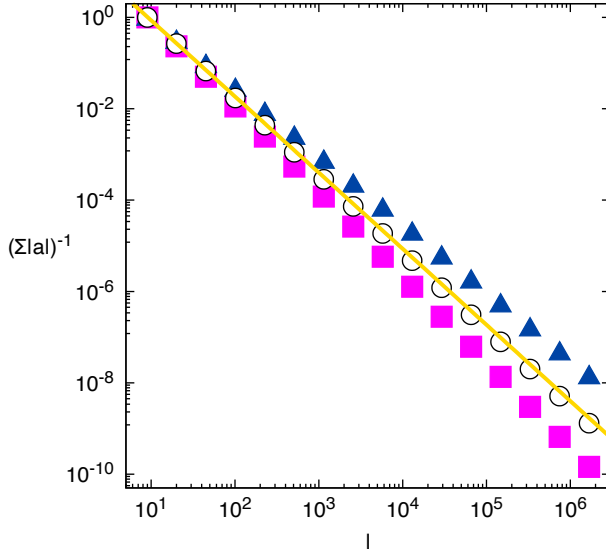


FIG. 6. Normalized results for $E(l_g) \equiv \left(\sum_{\forall a_i \neq 0} |a_i(l_g)| \right)^{-1}$. Points were calculated from the deterministic backbone with the same parameter values as in figure 3. In particular $a + b =$ (circles) $2,0225 \sim r_H$, (triangles) $1,871 < r_H$, and (squares) $(2,174 > r_H)$. The straight line is a power law with exponent $-\frac{5}{3}$, obtained when the deterministic system is almost tuned on the Hopf bifurcation critical point.

Preliminary results show departures from the power law with the noise turned on. However, in the present work, we have not analyzed this situation in full detail and prefer to leave it for a future publication.

XIII. DISCUSSION

The obtained $-5/3$ power law was obtained with exact calculation and not using a numerical approach. This result opens the possibility for turbulence energy cascades to be ruled by an analytical structure at least similar to rule (49, 50). In such a case, a possibility is that the quadratic nonlinearity in Eq. (1) could be capturing the intersecting dynamics of the Navier Stokes (NS) trajectories with a lower dimensional Poincare section. Then, rule (49, 50) would be the skeleton of the resulting intersection between higher dimensional trajectories and the lower dimensional dynamics given by Eq. (1). This skeleton would be carrying the main information shaping the energy spectrum in fully developed isotropic homogeneous turbulence.

Low dimensional dynamical systems have provided important insights into the onset of turbulence [32] and established a background on which improved understanding of turbulence has been achieved [9, 33, 34]. This work adds further evidence of the relevance of low dimensional discrete dynamics to understand turbulence. Furthermore, as intermittency and non-Gaussian statistics can be observed in many complex systems [35, 36] it may also be the case for $-5/3$ turbulent cascades, which our work indicates are not exclusive for fluids but a dynamical state rooted solely in critical deterministic nonlinear dynamics [33]. In particular, Eq. (1) is a specific case of a Lotka-Volterra system which have been shown to hold a winnerless competition [37] based multifractal neural coding scheme providing the first intrinsic neurodynamical explanation for wandering animal behavior [38]. Also, Eq. (1) can be related to SIR epidemic transmission dynamics [39], which may open the possibility for complex cascading phenomena in epidemic propagation.

Another crucial aspect derived from this work is whether rule (49, 50) is some sort of standard form for cascades or if it is an especial case of a more general principle. Whatever the case is, our work has shown that the discovered rule is general enough to produce the expected scaling for the turbulence energy spectrum and that it is a starting point to carry out further research on turbulent cascades from a novel point of view.

XIV. ACKNOWLEDGEMENTS

We thank Juan S. Medina-Álvarez for useful comments and discussions. JLCF and EDG acknowledges support from IVIC-141 grant during a small part of this work and personal support from Prof. M. C. Pereyra (UNM).

XV. AUTHOR CONTRIBUTIONS STATEMENT

JLCF conceived, directed, and developed all aspects of this research. MRM contributed with software development and simulation validations, EG independently validated the analytics. All authors contributed to paper writing. The authors declare no competing financial interests.

XVI. ADDITIONAL INFORMATION

Correspondence and requests for materials should be addressed to JLCF.

Appendix A: Eigenvalues of p_2

Let's calculate the second inner product, given by,

$$\begin{aligned}
p_2 &\equiv \mathbf{A}_{g-2}^\dagger p_1 \mathbf{A}_{g-2} = \\
&= \begin{bmatrix} \frac{r_2}{\beta} & 1 \\ -\alpha r_2 & 0 \end{bmatrix} \begin{bmatrix} \frac{r_1^2 + \beta^2}{\beta^2} & -\frac{r_1^2}{\beta} \alpha \\ -\frac{r_1^2}{\beta} \alpha & \alpha^2 r_1^2 \end{bmatrix} \begin{bmatrix} \frac{r_2}{\beta} & -\alpha r_2 \\ 1 & 0 \end{bmatrix} = \\
&= \begin{bmatrix} \frac{r_2^2 r_1^2 + r_2^2 \beta^2 - 2r_2 r_1^2 \alpha \beta^2 + r_1^2 \alpha^2 \beta^4}{\beta^4} & \frac{-r_2 r_1^2 - r_2 \beta^2 + r_1^2 \alpha \beta^2}{\beta^3} \alpha r_2 \\ \frac{-r_2 r_1^2 - r_2 \beta^2 + r_1^2 \alpha \beta^2}{\beta^3} \alpha r_2 & \alpha^2 r_2^2 \frac{r_1^2 + \beta^2}{\beta^2} \end{bmatrix},
\end{aligned} \tag{A1}$$

with eigenvalues,

$$\begin{aligned}
\lambda_{\pm}^{p_2} &= \frac{1}{2\beta^4} (r_2^2 r_1^2 + r_2^2 \beta^2 - 2r_2 r_1^2 \alpha \beta^2 + \beta^4 \alpha^2 r_1^2 + \beta^2 \alpha^2 r_2^2 r_1^2 + \beta^4 \alpha^2 r_2^2 \pm \\
&\quad (2r_2^4 r_1^2 \beta^2 + r_2^4 r_1^4 + r_2^4 \beta^4 + 2r_2^4 \beta^6 \alpha^2 + \beta^8 \alpha^4 r_1^4 + \beta^8 \alpha^4 r_2^4 - 4r_2 r_1^4 \alpha^3 \beta^6 \\
&\quad - 4r_2^3 r_1^4 \alpha^3 \beta^4 - 4r_2^3 r_1^2 \alpha^3 \beta^6 + 2\beta^6 \alpha^4 r_1^4 r_2^2 + \beta^4 \alpha^4 r_2^4 r_1^2 + 2\beta^6 \alpha^4 r_2^4 r_1^2 \\
&\quad - 2\beta^8 \alpha^4 r_1^2 r_2^2 - 4r_2^3 r_1^4 \alpha \beta^2 + 6r_2^2 r_1^4 \beta^4 \alpha^2 + 2r_2^4 r_1^4 \beta^2 \alpha^2 + 4r_2^4 r_1^2 \beta^4 \alpha^2 \\
&\quad - 4r_2^3 \beta^4 r_1^2 \alpha + 2r_2^2 \beta^6 \alpha^2 r_1^2)^{1/2}).
\end{aligned} \tag{A2}$$

Here, we can define,

$$\Lambda_2 \equiv \begin{bmatrix} (1 + \beta^2 \alpha^2) r_1^2 \\ + (\beta^2 + \beta^4 \alpha^2) \end{bmatrix} r_2^2 + \begin{bmatrix} (-2 \alpha \beta^2) r_1^2 \\ (\beta^4 \alpha^2) r_1^2 \end{bmatrix} r_2 + \begin{bmatrix} (\beta^4 \alpha^2) r_1^2 \\ (\beta^4 \alpha^2) r_1^2 \end{bmatrix}. \tag{A3}$$

It is easy to show that the term under the square root differs from Λ_2 by $4\alpha^4 r_2^2 r_1^2 \beta^8$. Then, we can make use of $\Upsilon_2 \equiv \sqrt{4\alpha^4 r_2^2 r_1^2 \beta^8} = 2\beta^4 \alpha^2 r_2 r_1$, to write the eigenvalues of p_2 as $\lambda_{\pm}^{p_2} = \frac{1}{2\beta^4} (\Lambda_2 \pm \sqrt{\Lambda_2^2 - \Upsilon_2^2})$.

Appendix B: Eigenvalues of p_3

The third inner product, given by,

$$\begin{aligned}
p_3 &= \mathbf{A}_{g-3}^\dagger p_2 \mathbf{A}_{g-3} = \\
&= \mathbf{A}_{g-3} \begin{bmatrix} \frac{r_2^2 r_1^2 + r_2^2 \beta^2 - 2r_2 r_1^2 \alpha \beta^2 + r_1^2 \alpha^2 \beta^4}{\beta^4} & \frac{-r_2 r_1^2 - r_2 \beta^2 + r_1^2 \alpha \beta^2}{\beta^3} \alpha r_2 \\ \frac{-r_2 r_1^2 - r_2 \beta^2 + r_1^2 \alpha \beta^2}{\beta^3} \alpha r_2 & \alpha^2 r_2^2 \frac{r_1^2 + \beta^2}{\beta^2} \end{bmatrix} \mathbf{A}_{g-3},
\end{aligned} \tag{B1}$$

has eigenvalues that can be written as $\lambda_{\pm}^{p_3} = \frac{1}{2\beta^6} \left(\Lambda_3 \pm \sqrt{\Lambda_3^2 - \Upsilon_3^2} \right)$, where,

$$\Lambda_3 \equiv \left\{ \begin{array}{l} \left[(1 + \beta^2 \alpha^2) r_1^2 \right] r_2^2 \\ + \left[(\beta^2 + \beta^4 \alpha^2) \right] r_2 \\ + \left[(-2 \alpha \beta^2 - 2 \beta^4 \alpha^3) r_1^2 \right] r_2 \\ + \left[(\beta^4 \alpha^2 + \beta^6 \alpha^4) r_1^2 \right] \end{array} \right\} r_3^2 + \left\{ \begin{array}{l} \left[(-2 \alpha \beta^2) r_1^2 \right] r_2^2 \\ + \left[(-2 \alpha \beta^4) \right] r_3 \\ + \left[(2 \alpha^2 \beta^4) r_1^2 \right] r_2 \end{array} \right\} r_3 + \left\{ \begin{array}{l} \left[(\beta^4 \alpha^2) r_1^2 \right] r_2^2 \\ + \left[(\alpha^2 \beta^6) \right] \end{array} \right\} \quad (B2)$$

and $\Upsilon_3 = 2\beta^6 \alpha^3 r_3 r_2 r_1$.

Appendix C: Eigenvalues of p_4

The fourth inner product becomes,

$$p_4 = \mathbf{A}_{g-4}^\dagger p_3 \mathbf{A}_{g-4} \quad (C1)$$

with eigenvalues $\lambda_{\pm}^{p_4} = \frac{1}{2\beta^8} \left(\Lambda_4 \pm \sqrt{\Lambda_4^2 - \Upsilon_4^2} \right)$, where,

$$\Lambda_4 \equiv \left\{ \begin{array}{l} \left[(1 + \beta^2 \alpha^2) r_1^2 \right] r_2^2 \\ + \left[(\beta^2 + \beta^4 \alpha^2) \right] r_2 \\ + \left[(-2 \beta^4 \alpha^3 - 2 \alpha \beta^2) r_1^2 \right] r_2 \\ + \left[(\beta^6 \alpha^4 + \beta^4 \alpha^2) r_1^2 \right] \end{array} \right\} r_3^2 + \left\{ \begin{array}{l} \left[(-2 \beta^4 \alpha^3 - 2 \alpha \beta^2) r_1^2 \right] r_2^2 \\ + \left[(-2 \beta^6 \alpha^3 - 2 \alpha \beta^4) \right] r_3 \\ + \left[(2 \beta^6 \alpha^4 + 2 \beta^4 \alpha^2) r_1^2 \right] r_2 \end{array} \right\} r_3 + \left\{ \begin{array}{l} \left[(\beta^6 \alpha^4 + \beta^4 \alpha^2) r_1^2 \right] r_2^2 \\ + \left[(\beta^8 \alpha^4 + \alpha^2 \beta^6) \right] \end{array} \right\} r_2^2 \quad (C2)$$

$$\begin{aligned}
& + \left(\begin{array}{c} \left\{ \begin{array}{c} \left[(-2\alpha\beta^2)r_1^2 \right] r_2^2 \\ + (-2\alpha\beta^4) \end{array} \right\} r_3^2 \\ + \left[(4\alpha^2\beta^4)r_1^2 \right] r_2 \\ + \left[(-2\alpha^3\beta^6)r_1^2 \right] \end{array} \right) r_4 \\
& + \left(\begin{array}{c} \left\{ \begin{array}{c} \left[(2\beta^4\alpha^2)r_1^2 \right] r_2^2 \\ + (2\alpha^2\beta^6) \end{array} \right\} r_3 \\ + \left[(-2\alpha^3\beta^6)r_1^2 \right] r_2 \end{array} \right) \\
& + \left(\begin{array}{c} \left\{ \begin{array}{c} \left[(\beta^4\alpha^2)r_1^2 \right] r_2^2 \\ + (\alpha^2\beta^6) \end{array} \right\} r_3^2 \\ + \left[(-2\alpha^3\beta^6)r_1^2 \right] r_2 \\ + \left[(\alpha^4\beta^8)r_1^2 \right] \end{array} \right)
\end{aligned}$$

and $\Upsilon_4 = 2\beta^8\alpha^4r_4r_3r_2r_1$.

Appendix D: Eigenvalues of p_5

Here we show p_5 , given by,

$$p_5 = \mathbf{A}_{g-5}^\dagger p_4 \mathbf{A}_{g-5}, \quad (D1)$$

with eigenvalues, $\lambda_{\pm}^{p_5} = \frac{1}{2\beta^{10}} \left(\Lambda_5 \pm \sqrt{\Lambda_5^2 - \Upsilon_5^2} \right)$, with,

$$\begin{aligned}
\Lambda_5 \equiv & \left[\left(\left\{ \begin{array}{l} (1 + \beta^2 \alpha^2) r_1^2 \\ + (\beta^2 + \beta^4 \alpha^2) \end{array} \right\} r_2^2 \right) r_3^2 \right. \\
& + \left. \left\{ \begin{array}{l} (-2 \alpha \beta^2 - 2 \beta^4 \alpha^3) r_1^2 \\ + (\beta^4 \alpha^2 + \beta^6 \alpha^4) r_1^2 \end{array} \right\} r_2 \right\} r_4^2 \\
& + \left\{ \begin{array}{l} (-2 \alpha \beta^2 - 2 \beta^4 \alpha^3) r_1^2 \\ + (-2 \beta^6 \alpha^3 - 2 \alpha \beta^4) \end{array} \right\} r_2^2 \left. \right\} r_3 \\
& + \left\{ \begin{array}{l} (2 \beta^6 \alpha^4 + 2 \beta^4 \alpha^2) r_1^2 \\ + (\beta^4 \alpha^2 + \beta^6 \alpha^4) r_1^2 \end{array} \right\} r_2^2 \\
& + \left\{ \begin{array}{l} + (\beta^8 \alpha^4 + \alpha^2 \beta^6) \end{array} \right\} r_2^2 \\
& \left. \left\{ \begin{array}{l} (-2 \alpha \beta^2 - 2 \beta^4 \alpha^3) r_1^2 \\ + (-2 \beta^6 \alpha^3 - 2 \alpha \beta^4) \end{array} \right\} r_2^2 \right\} r_3^2 \left. \right\} r_5^2 \quad (D2) \\
& + \left. \left\{ \begin{array}{l} (4 \beta^6 \alpha^4 + 4 \beta^4 \alpha^2) r_1^2 \\ + (-2 \beta^6 \alpha^3 - 2 \beta^8 \alpha^5) r_1^2 \end{array} \right\} r_2 \right\} r_4 \\
& + \left\{ \begin{array}{l} (2 \beta^6 \alpha^4 + 2 \beta^4 \alpha^2) r_1^2 \\ + (2 \beta^8 \alpha^4 + 2 \alpha^2 \beta^6) \end{array} \right\} r_2^2 \left. \right\} r_3 \\
& + \left\{ \begin{array}{l} + (-2 \beta^6 \alpha^3 - 2 \beta^8 \alpha^5) r_1^2 \end{array} \right\} r_2 \left. \right\} r_3^2 \\
& + \left. \left\{ \begin{array}{l} (\beta^4 \alpha^2 + \beta^6 \alpha^4) r_1^2 \\ + (\beta^8 \alpha^4 + \alpha^2 \beta^6) \end{array} \right\} r_2^2 \right\} r_3^2 \\
& + \left. \left\{ \begin{array}{l} + (-2 \beta^6 \alpha^3 - 2 \beta^8 \alpha^5) r_1^2 \\ + (\beta^8 \alpha^4 + \beta^{10} \alpha^6) r_1^2 \end{array} \right\} r_2 \right\} r_3^2
\end{aligned}$$

$$\begin{aligned}
& + \left[\left(\begin{array}{l} \left\{ \begin{array}{l} \left[(-2\alpha\beta^2)r_1^2 \right] r_2^2 \\ + (-2\alpha\beta^4) \end{array} \right\} r_3^2 \\ + \left[(4\alpha^2\beta^4)r_1^2 \right] r_2 \\ + \left[(-2\alpha^3\beta^6)r_1^2 \right] \end{array} \right) r_4^2 \right. \\
& \quad \left. + \left\{ \begin{array}{l} \left[(4\beta^4\alpha^2)r_1^2 \right] r_2^2 \\ + (4\alpha^2\beta^6) \\ + \left[(-4\alpha^3\beta^6)r_1^2 \right] r_2 \end{array} \right\} r_3 + \left[\begin{array}{l} (-2\alpha^3\beta^6)r_1^2 \\ (-2\alpha^3\beta^8) \end{array} \right] r_2^2 \right\} r_5 \\
& + \left[\left(\begin{array}{l} \left\{ \begin{array}{l} \left[(2\beta^4\alpha^2)r_1^2 \right] r_2^2 \\ + (2\alpha^2\beta^6) \end{array} \right\} r_3^2 \\ + \left[(-4\alpha^3\beta^6)r_1^2 \right] r_2 \\ + \left[(2\alpha^4\beta^8)r_1^2 \right] \end{array} \right) r_4 \right. \\
& \quad \left. + \left\{ \begin{array}{l} \left[(-2\alpha^3\beta^6)r_1^2 \right] r_2^2 \\ + (-2\alpha^3\beta^8) \\ + \left[(2\alpha^4\beta^8)r_1^2 \right] r_2 \end{array} \right\} r_3 \right\} r_4 \\
& + \left[\left(\begin{array}{l} \left\{ \begin{array}{l} \left[(\beta^4\alpha^2)r_1^2 \right] r_2^2 \\ + (\alpha^2\beta^6) \end{array} \right\} r_3^2 \\ + \left[(-2\alpha^3\beta^6)r_1^2 \right] r_2 \\ + \left[(\alpha^4\beta^8)r_1^2 \right] \end{array} \right) r_4^2 \right. \\
& \quad \left. + \left\{ \begin{array}{l} \left[(-2\alpha^3\beta^6)r_1^2 \right] r_2^2 \\ + (-2\alpha^3\beta^8) \\ + \left[(2\alpha^4\beta^8)r_1^2 \right] r_2 \end{array} \right\} r_3 \right. \\
& \quad \left. + \left\{ \begin{array}{l} \left[(\alpha^4\beta^8)r_1^2 \right] r_2^2 \\ + (\alpha^4\beta^{10}) \end{array} \right\} \right] r_4^2
\end{aligned}$$

and $\Upsilon_5 = 2\beta^{10}\alpha^5 r_5 r_4 r_3 r_2 r_1$.

[1] L. F. Richardson, Proceedings of the Royal Society of London Series A **110**, 709 (1926).

[2] A. N. Kolmogorov, Soviet Physics Uspekhi **10**, 734 (1968).

- [3] G. L. Eyink and K. R. Sreenivasan, Rev. Mod. Phys. **78**, 87 (2006).
- [4] A. M. Obukhov, Dok. Akad. Nauk. SSSR **32**, 22 (1941).
- [5] L. Onsager, Phys. Rev. **68**, 286 (1945).
- [6] W. Heisenberg, Zeitschrift für Physik **124**, 628 (1948).
- [7] C. F. v. Weizsäcker, Zeitschrift für Physik **124**, 614 (1948).
- [8] L. Biferale, M. Blank, and U. Frisch, Journal of Statistical Physics **75**, 781 (1994).
- [9] U. Frisch, *Turbulence: The Legacy of A. N. Kolmogorov* (Cambridge University Press, 1995).
- [10] K. R. Sreenivasan, The Physics of Fluids **27**, 1048 (1984).
- [11] A. La Porta, G. A. Voth, A. M. Crawford, J. Alexander, and E. Bodenschatz, Nature **409**, 1017 (2001).
- [12] P. W. Hammer, N. Platt, S. M. Hammel, J. F. Heagy, and B. D. Lee, Phys. Rev. Lett. **73**, 1095 (1994).
- [13] F. Rödelsperger, A. Čenys, and H. Benner, Phys. Rev. Lett. **75**, 2594 (1995).
- [14] C.-S. Poon and C. K. Merrill, Nature **389**, 492 (1997).
- [15] D. L. Feng, C. X. Yu, J. L. Xie, and W. X. Ding, Phys. Rev. E **58**, 3678 (1998).
- [16] A. Krawiecki, J. A. Holyst, and D. Helbing, Phys. Rev. Lett. **89**, 158701 (2002).
- [17] J. L. Cabrera and J. G. Milton, Phys. Rev. Lett. **89**, 158702 (2002).
- [18] A. Veltri and V. Carbone, Phys. Rev. Lett. **92**, 143901 (2004).
- [19] E. A. Spiegel, Chaos and intermittency in the solar cycle (Springer New York, New York, NY, 2009) pp. 25–51.
- [20] F. Freyer, K. Aquino, P. A. Robinson, P. Ritter, and M. Breakspear, The Journal of Neuroscience **29**, 8512 (2009).
- [21] H. Yang and E. Ding, Phys. Rev. E **50**, R3295 (1994).
- [22] Y. Morimoto, Physics Letters A **134**, 179 (1988).
- [23] J. L. Cabrera and F. J. de la Rubia, Physics Letters A **197**, 19 (1995).
- [24] J. L. Cabrera and F. J. de la Rubia, International Journal of Bifurcation and Chaos **06**, 1683 (1996).
- [25] J. Maynard Smith, *Mathematical Ideas in Biology* (Cambridge University Press, 1968).
- [26] D. G. Aronson, M. A. Chory, G. R. Hall, and R. P. McGehee, Communications in Mathematical Physics **83**, 303 (1982).
- [27] J. R. Pounder and T. D. Rogers, Bulletin of Mathematical Biology **42**, 551 (1980).

- [28] J. L. Cabrera and F. J. d. l. Rubia, *Europhys. Lett.* **39**, 123 (1997).
- [29] J. L. Cabrera, J. Gorroñogoitia, and F. J. de la Rubia, *Phys. Rev. Lett.* **82**, 2816 (1999).
- [30] V. Trifonov, L. Pasqualucci, R. Dalla-Favera, and R. Rabadan, *Scientific Reports* **1**, 191 (2011).
- [31] S. G. Saddoughi and S. V. Veeravalli, *J. Fluid Mechanics* **268**, 333 (1994).
- [32] J. P. Eckmann, *Rev. Mod. Phys.* **53**, 643 (1981).
- [33] T. Bohr, M. H. Jensen, G. Paladin, and A. Vulpiani, *Dynamical Systems Approach to Turbulence* (Cambridge University Press, Cambridge, 1998).
- [34] J. M. McDonough, *Phys. Rev. E* **79**, 065302 (2009).
- [35] J. L. Cabrera and J. G. Milton, *Chaos: An Interdisciplinary Journal of Nonlinear Science* **14**, 691 (2004).
- [36] R. N. Mantegna and H. E. Stanley, *Nature* **376**, 46 (1995).
- [37] L. A. González-Díaz, E. D. Gutiérrez, P. Varona, and J. L. Cabrera, *Phys. Rev. E* **88**, 012709 (2013).
- [38] E. D. Gutiérrez and J. L. Cabrera, *Scientific Reports* **5**, 18009 (2015).
- [39] L. J. Allen, *Mathematical Biosciences* **124**, 83 (1994).